PHYSICAL REVIEW B VOLUME 51, NUMBER 6 1 FEBRUARY 1995-II

Microscopic magnetization reversal processes and magnetic domain structure in epitaxial Fe/GaAs(001) films

E. Gu, J. A. C. Bland, C. Daboo, M. Gester, and L. M. Brown
Cavendish Laboratory, University of Cambridge, Madingley Road, Cambridge CB3 0HE, United Kingdom

R. Ploessl and J. N. Chapman
Department of Physics and Astronomy, University of Glasgow, Glasgow G12 8QQ, United Kingdom
(Received 25 March 1994; revised manuscript received 24 October 1994)

We report the results of Lorentz electron microscopy studies of the microscopic magnetic reversal behavior of epitaxial Fe/GaAs(001) thin films in the thickness range 150–450 Å in order to explain how the microscopic processes give rise to the observed macroscopic reversal behavior. The results are described in the context of scanning tunneling microscopy and transmission electron microscopy studies of the film microstructure and of magneto-optical Kerr effect magnetometry studies of the macroscopic magnetic switching behavior. We find that striking differences in the domain structure occur according to the crystallographic direction along which the field is applied. For applied fields aligned close to the in-plane ⟨110⟩ directions (hard axes), magnetization reversal proceeds via a combination of coherent rotation and displacements of 90° domain walls aligned along the ⟨110⟩ directions. For magnetization reversal along the in-plane ⟨100⟩ directions (easy axes), an irregular checkerboard domain structure develops at the transition field: well-defined 90° and 180° domain walls coexist, aligned along the ⟨110⟩ and ⟨100⟩ directions, respectively. The magnetization reversal along the ⟨100⟩ directions takes place via a combination of domain nucleation and wall displacements. The magnetic reversal of unfavorably oriented domains is found to occur by a combination of two 90° reorientations.

I. INTRODUCTION

Single-crystal Fe films grown epitaxially on semiconductor substrates offer an opportunity to realize an artificial low-dimensional system with controllable magnetic properties, offering possibilities for a range of device applications,[1] while also permitting fundamental studies in magnetism.[2–7] Recently, the longitudinal and transverse magneto-optical Kerr effects (MOKE) have been used to study the macroscopic magnetization reversal process in epitaxial Fe/GaAs(001) thin films.[7–9] In the present paper we shall clarify how the microscopic processes give rise to the observed macroscopic reversal behavior.

To date very few studies of the domain structure as a function of field have been carried out for such in-plane anisotropy epitaxial films (for which the remanent magnetization lies in-plane) due to the technical difficulties associated with measuring weak magnetic contrast in finite applied fields. Domain imaging studies have been carried out in zero applied field for both ultrathin[10–13] and thick[14–16] epitaxial transition metal films with in-plane anisotropy. The theoretically predicted single-domain state for a two-dimensional (2D) in-plane anisotropy film[10] has been observed for as-grown ultrathin Co/Cu(100) films.[13] In contrast, for thicker ($t \sim 500$ Å) Fe/MgO(100) films a checkerboard domain pattern made up of only 90° walls was realized in the demagnetized state.[15] These results illustrate that the thickness dependence of the magnetostatic energy is important in giving rise to the domain structure.

By using the technique of molecular-beam epitaxy (MBE) and employing a high-quality single-crystal semiconductor as a substrate, it is now possible to prepare epitaxial Fe films with well defined magnetic properties.[4,7] The high-quality substrate and MBE technique are appropriate in the present context since the earlier studies of Fe/MgO showed that the magnetic domain structures were influenced greatly by the steps and tear lines on the MgO substrate surface[14] indicating that high sample quality is essential for domain imaging studies. For MBE grown epitaxial Fe/GaAs(001) films with in-plane anisotropy, the domain evolution as a function of applied field and how this evolution is influenced by film anisotropy properties have not been studied previously. In this work, the microstructure and microscopic magnetization reversal processes in such films are studied by using transmission electron microscopy (TEM), scanning tunneling microscopy (STM), magneto-optical Kerr effect (MOKE) magnetometry and a Lorentz TEM microscope. We have chosen to study Fe/GaAs(001) films in the thickness range 150–450 Å since for these thicker films, the contribution of surface defects and atomic steps may be expected to be less important than in the ultrathin case. We shall show that for such films the single-domain state predicted for a 2D film is also the lowest energy state at zero field. We find that well-defined domain structures develop at transition fields. These structures are qualitatively different not only from those of ultrathin films[17] but also from those of the bulk.

0163-1829/95/51(6)/3596(9)/$06.00 ©1995 The American Physical Society

II. EXPERIMENTAL DETAILS

A. Preparation of Lorentz TEM specimens

In this work, Fe films deposited on GaAs substrates were investigated by TEM and Lorentz TEM. TEM specimens must be sufficiently thin so as to permit the transmission of electrons. To obtain such thin TEM specimens, ion-beam milling and film stripping techniques are generally used. However, for magnetic domain studies, in order to avoid the influence of stray fields on the domain structures, the area studied should be far from the sample edge and for the observation of domain evolution, it should be at least 50 μm$\times$50 μm in size. Therefore it is desirable to form an electron transparent window in the center of samples. It is generally impossible to produce such a large uniform window specimen by conventional preparative techniques. As an alternative, a new selective chemical etching technique was used. In this work, $Ga_{0.7}Al_{0.3}As$ which was epitaxially grown on a GaAs(001) wafer was employed as an etch stop layer.[18] A 50-nm-thick GaAs layer (membrane) was then epitaxially grown on this etch stop layer. In order to protect the GaAs layer against contamination, an As cap layer was deposited on its surface. This As cap layer was desorbed before film deposition. After film growth, the film together with the GaAs(001) membrane suitable for TEM observation was formed by selective chemical etching from the back surface of the GaAs wafer through an etching window. The cross section of completed Lorentz TEM specimens is shown schematically in Fig. 1.

B. Film growth and structural characterization

The epitaxial Fe films were grown in a UHV chamber. During growth, the pressure was less than 5×10^{-10} mbar. The film thickness was monitored by a quartz microbalance calibrated by a Dektak profilometer. The As cap layer on the GaAs(001) membrane was desorbed before the film growth by annealing at 510 °C so as to get a clean and ordered GaAs surface.[19] The optimum substrate temperature of 150 °C and a deposition rate of 1 Å min^{-1} were used for the Fe growth. During growth, the surface structure was monitored by low-energy electron diffraction (LEED). LEED patterns confirm the epitaxial growth of bcc Fe. However, broad LEED diffraction spots from the Fe layers indicate an irregular step surface, i.e., the Fe growth departs from an ideal layer by layer two-dimensional growth mode. Finally, to prevent oxidation, each Fe film was covered by a Cr coating.

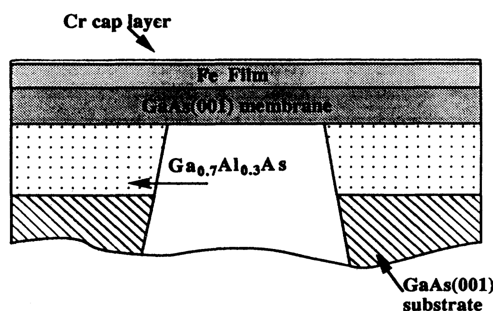

FIG. 1. Cross-section of the Lorentz TEM specimens prepared by selective chemical etching technique.

The surface topographic images of the completed films and GaAs substrates were revealed *ex situ* by a Nanoscope II STM with electrochemically etched tungsten tips. Microstructural analysis of the Fe films was performed by a JEOL-2000EX electron microscope operated at 200 kV.

C. MOKE magnetometric measurements and Lorentz microscopy

The detailed macroscopic magnetization reversal behavior of the Fe films was studied *ex situ* using a MOKE magnetometer.[8,20] The MOKE technique used here measures *M-H* Loops for two orientations of the in-plane applied field, namely parallel and perpendicular to the plane of incidence of the light. From the resulting loops, the $M_{\parallel}$ and $M_{\perp}$ components of the relative in-plane magnetization (M/M_s) can be determined directly.[20]

The micromagnetic domain structure in the Fe films was revealed using a Lorentz electron microscope equipped with a magnetizing stage.[21] After mounting in the stage, the specimens can be rotated about a vertical axis by an external drive so that the field can be applied in any in-plane direction with respect to the specimen. The Foucault mode of Lorentz electron microscopy was used in this work.[21,22] For the Foucault mode, a pair of images sensitive to orthogonal components of magnetization are required to produce a map of the in-plane magnetization distribution across the film sample. In our measurements the components parallel and perpendicular to the applied field direction were always mapped.

III. RESULTS AND DISCUSSION

A. Structure and surface morphology

A typical electron-diffraction pattern of Fe/GaAs(001) films is shown in Fig. 2(a). This diffraction pattern can be indexed as shown in Fig. 2(b). It can be seen that the 200-type diffraction spots from the GaAs are very sharp and the 220- and 400-type diffraction spots from the GaAs are broad and elongated. Since the lattice constant of bulk bcc Fe is approximately half that of GaAs which has a zinc-blende structure, the broad and elongated diffraction spots shown in Fig. 2 are due to the overlap of diffraction patterns from the GaAs and the bcc Fe layer. As 100-type diffractions are forbidden for elements with a bcc structure, like Fe, the spot broadening does not occur for the 200 diffraction spots of GaAs. These results confirm directly the epitaxial growth of bcc Fe on the GaAs(001) substrate. The epitaxial relationship is Fe(001)‖GaAs(001) and Fe[110]‖GaAs[110], i.e., the Fe(001) surface net forms a $c(1\times1)$ structure on the GaAs(001) surface.

The surface topography of the Fe films was investigated by STM to determine whether the magnetic domain structure reflects the presence of surface topological features. An STM image of an Fe(150 Å)/GaAs(001) film is shown in Fig. 3. Although the film is highly epitaxial, it reveals that the surface of the film has islandlike undulations about 10 Å high and about 150 Å in diameter. A large concave area about 10 Å deep can be seen in this image. It is likely that this feature is produced by the substrate since similar features have also been observed on the surface of the substrate prior to film deposition.

From our LEED and STM measurements, it is clear that the Fe growth on As-desorbed GaAs(001) departs from an ideal layer by layer two-dimensional growth mode. Three-dimensional growth has also been found in the growth of Fe on oxide-desorbed GaAs(001) by Jonker, Prinz, and Idzerda using electron forward-scattering techniques.[23] Nevertheless, electron-diffraction results show that there is a well-defined relation between the orientation of the Fe and the crystallographic axes of the GaAs substrate throughout the film.

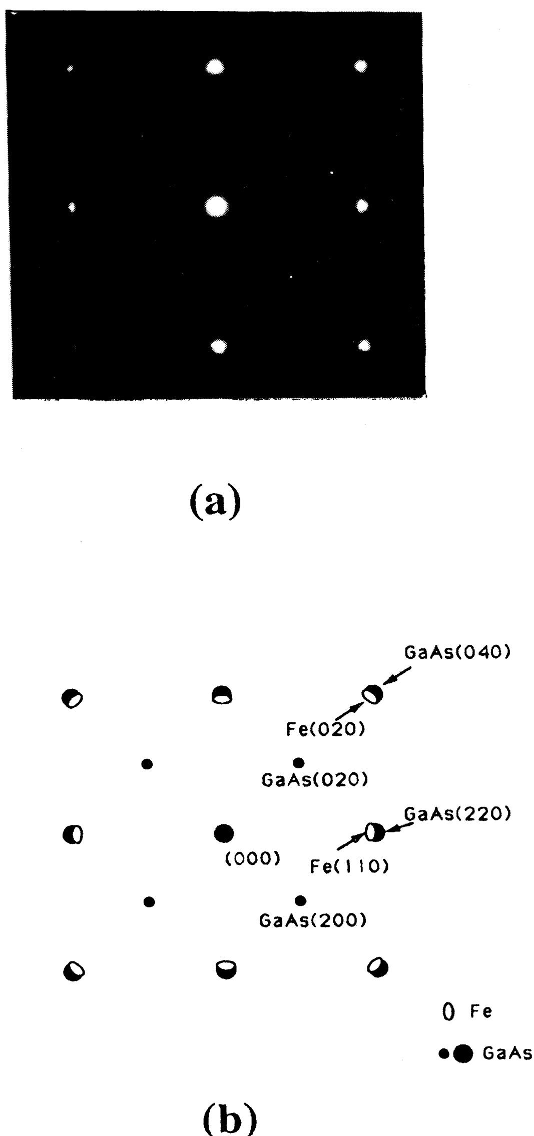

FIG. 2. (a) A typical selected-area electron-diffraction pattern of Fe/GaAs (001) films, (b) A schematic indexed pattern corresponding to the diffraction pattern shown in (a).

B. Macroscopic magnetic switching behavior

MOKE hysteresis loops of the Fe(150 Å)/GaAs(001) film are shown for the applied field aligned parallel to the ⟨110⟩ in-plane hard direction in Figs. 4(a) and 4(b) and parallel to the ⟨100⟩ in-plane easy direction in Figs. 4(c) and 4(d). For these loops, the Kerr signal intensity is proportional to the component of magnetization parallel to the applied field (longitudinal geometry). The detailed minor MOKE hysteresis loops shown in Figs. 4(b) and 4(d) were measured by scanning the field up to 30 Oe. It can be seen that when the field is applied along the ⟨110⟩ direction, initially there is a gradual decrease of the $M_{\|}$ component from saturation as the field strength is reduced from the saturation value. An abrupt jump occurs at a small negative field [4.8 Oe in Fig. 4(b)] followed by a further gradual decrease until negative saturation is reached. MOKE loops obtained for the component of the magnetization perpendicular to the applied field direction confirm that a coherent rotation of the magnetization occurs beyond the transition fields.[8] In contrast, along the ⟨100⟩ direction, the magnetization switches [at a field of 7.0 Oe in Fig. 4(d)] directly between saturated states. However, in both cases Barkhausen discontinuities are observed clearly in the minor MOKE hysteresis loops indicative of the irreversible movement of domain walls at the transition fields.[24]

C. Magnetic domain structure and magnetization reversal processes

1. ⟨110⟩ hard directions

To carry out reproducible domain studies it is important that the initial magnetic state is well defined. Firstly, a single-domain state of the Fe(150 Å)/GaAs(001) film was induced in the Lorentz electron microscope by applying a magnetic field H_i ($H_i = 120$ Oe) along one of the ⟨110⟩ directions as determined from the diffraction pattern, say the $[1\bar{1}0]$ direction. Then the field was reduced to zero. In the remanent state, the Fe film is found to be still in a single-domain configuration. This single-domain state persisted up to a critical reverse field strength $H_r = H^h_{\rm crit}$ ($H^h_{\rm crit} = 5.6$ Oe for the field amplitude $H_i = 120$ Oe) applied along the $[\bar{1}10]$ direction at which domain walls were first observed. Only a few domain walls, extending several hundreds of microns across the whole area of the window, appeared. By comparing the microscopic magnetization reversal behavior with the macroscopic behavior determined from MOKE, we are able to identify the field strength ($H^h_{\rm crit}$) at which the domain walls appear to the transition field determined from the M-H loop. A Foucault image, sensitive to the component of induction parallel to the field direction and recorded at the critical field strength is shown in Fig. 5(a). In this image, a single wall running almost parallel to the $[\bar{1}10]$

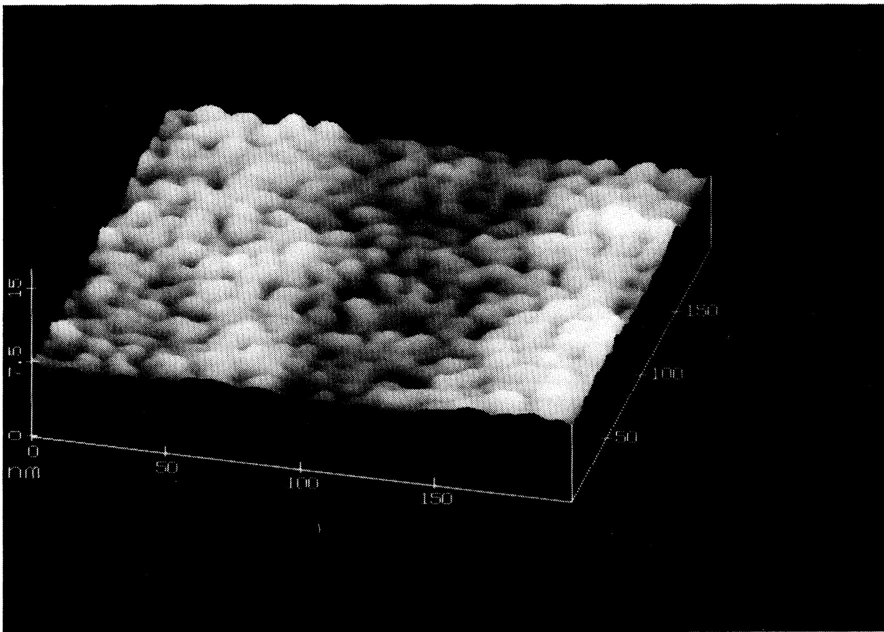

FIG. 3. Scanning tunneling microscope image of an Fe(150 Å)/GaAs(001) film.

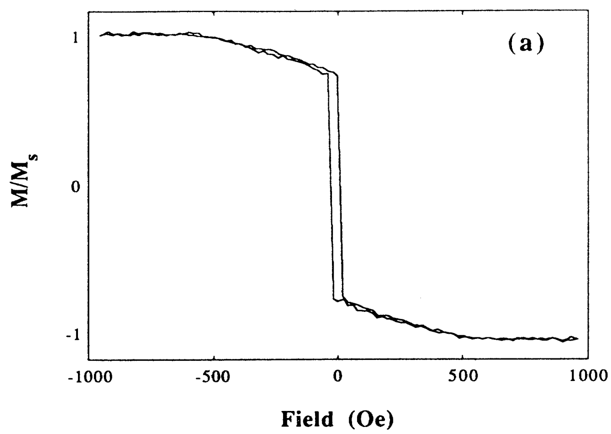

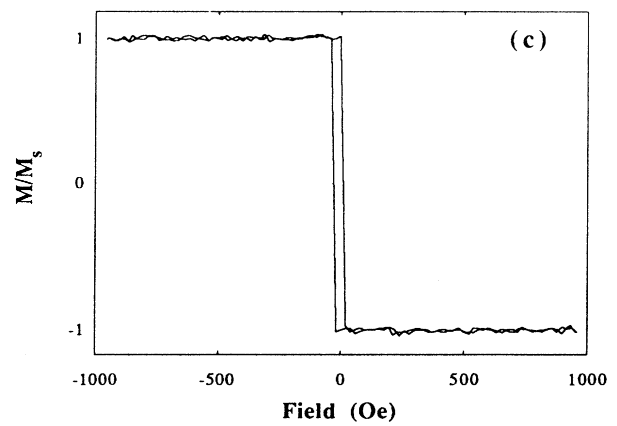

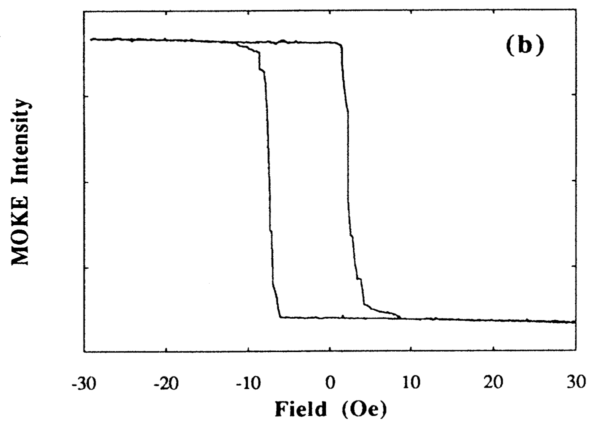

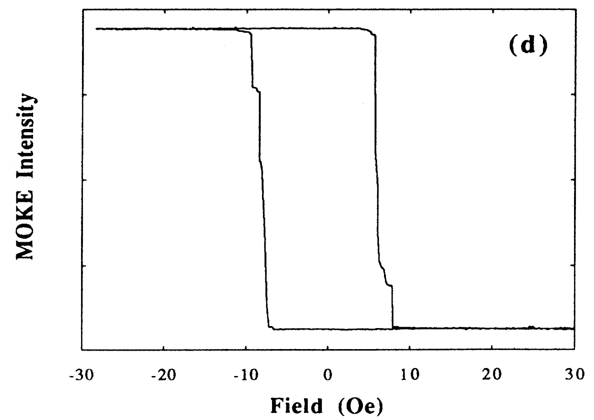

FIG. 4. MOKE hysteresis loops for the Fe (150 Å)/GaAs(001) film. The field is applied parallel to the in-plane ⟨110⟩ hard direction (a) for fields up to saturation and (b) for a field amplitude of 30 Oe. Equivalent loops obtained for the in-plane ⟨100⟩ easy direction are shown in (c) and (d).

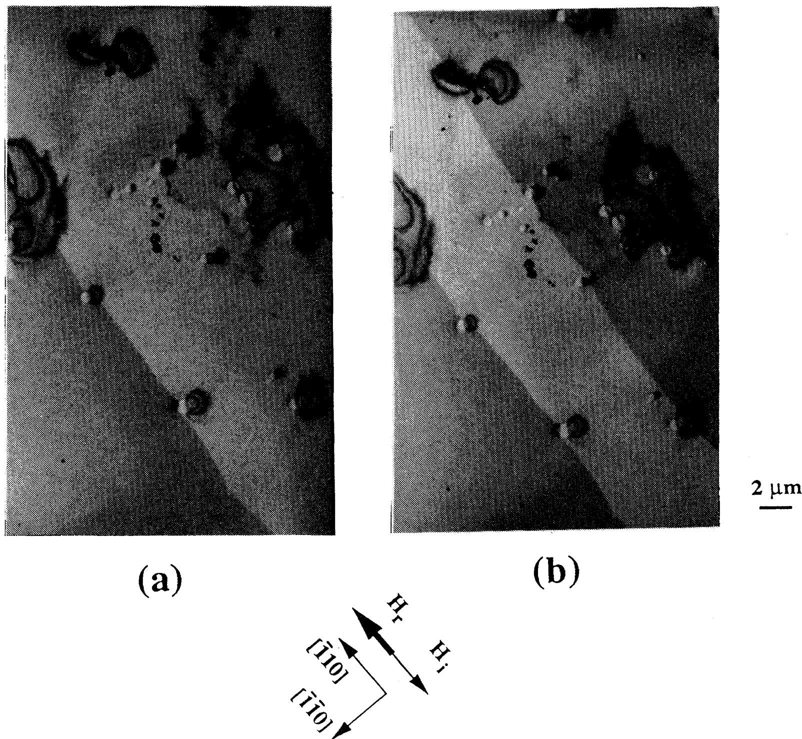

FIG. 5. Foucault images of the Fe(150 Å)/GaAs(001) film for the field applied along the hard axis. The components of induction mapped were parallel to the applied magnetic field direction for reverse field strengths ($H_r \| [\bar{1}10]$) of (a) $H^h_{\rm crit}$, (b) $1.10 H^h_{\rm crit}$. Note the defects pinning the domain walls.

direction can be seen. Figure 5(b) shows what happened when the field strength was increased to a value of 1.10 $H^h_{\rm crit}$. In this case the domain wall seen in Fig. 5(a) remained pinned at the original position but another domain wall moved into the field of view from the top right-hand corner. A further small increase of field led to the disappearance of domain walls from the whole of the visible area of the sample. Repetition of the field cycle described above showed that the fields at which walls appeared and disappeared were highly reproducible. Furthermore, it was noted that Foucault images sensitive to the component of induction perpendicular to the field direction were never found to show contrast variations, indicative of a constant (or zero) magnetization component in that direction. The Foucault images shown in Fig. 5 thus are consistent with either the magnetization distribution shown schematically in Figs. 6(a)–6(d) or that shown in Figs. 6(e)–6(h).

The overall magnetization reversal process for fields along the ⟨110⟩ direction can now be explained with reference to Fig. 7. Whilst [1$\bar{1}$0] lies midway between the easy [100] and [0$\bar{1}$0] directions, in practice, the applied field will never be exactly along the intended direction. As the field strength is reduced from a high value along a direction close to the [1$\bar{1}$0] axis, the magnetization coherently rotates towards the nearest easy axis ([100] in Fig. 7). Hence, in the remanent state, the sample is uniformly magnetized as a single domain along this "preferred" easy direction. Application of a field of the opposite polarity (namely one parallel to [$\bar{1}$10]) leaves the film in its single-domain state until, at the critical field, 90° walls are nucleated and these sweep across the specimen introducing domains in which the magnetization is oriented along [010], the easy direction near to that of the applied field. Increasing the field strength by only a fraction of 1 Oe allows [010]-oriented domains to grow through Barkhausen-like jumps, the jump distance being of the order of a few tens of microns as judged directly from observations on the TEM screen. The jump direction is along [$\bar{1}\,\bar{1}$0]. When it is complete the whole of the film is once again uniformly magnetized but the

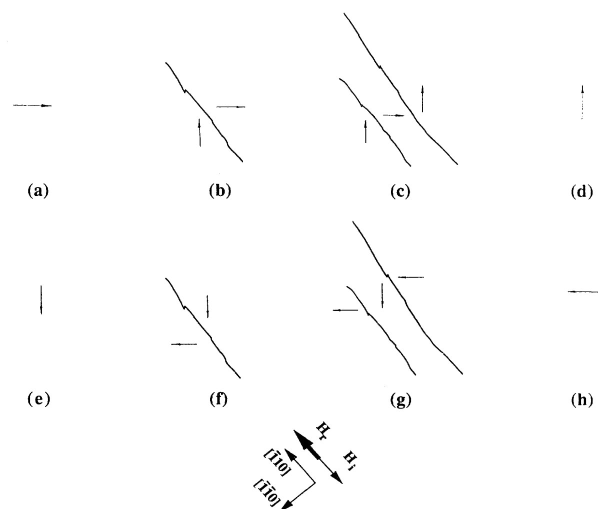

FIG. 6. Schematic diagram of two possible magnetization distributions deduced from Fig. 5. The reverse field corresponds to strengths of (a), (e) 0.0 Oe, (b), (f) $H^h_{\rm crit}$, (e), (g) 1.10 $H^h_{\rm crit}$, (d), (h) 1.18 $H^h_{\rm crit}$.

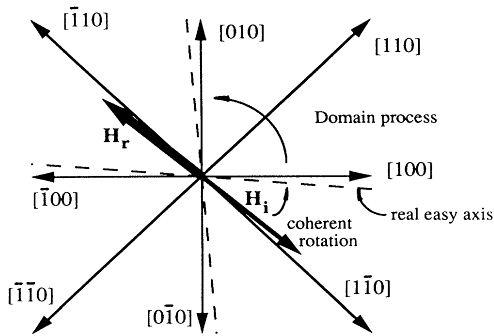

FIG. 7. Magnetization reversal process for applied fields near the ⟨110⟩ direction.

direction of magnetization has changed from being along [100] to lying along [010]. The domain-wall jump observed gives rise to the sharp 90° change of the macroscopic magnetization deduced from MOKE measurements.[8] Increasing the field strength further leads to rotation of the magnetization away from the [010] direction towards that of the applied field. The description given above is in accord with the magnetization distributions shown in Figs. 6(a)–6(d). If the applied field was initially closer to [0$\bar{1}$0] rather than to [100] similar processes would be involved although domain-wall motion would now take the sample from a uniformly magnetized state parallel to [0$\bar{1}$0] to one parallel to [$\bar{1}$00]. In this instance the magnetization distributions would be as shown in Figs. 6(e)–6(h). Very similar magnetization reversal behavior has also been observed for an Fe(450 Å)/GaAs(001) film along the ⟨110⟩ hard directions, with the displacement of domain walls occurring along the ⟨110⟩ direction.

The presence of only a cubic magnetic anisotropy is assumed in the analysis given above. In practice, for thin Fe/GaAs(001) films, an additional uniaxial anisotropy always exists and the strength of this uniaxial anisotropy depends on film thickness.[25] If the uniaxial anisotropy is taken into account, the real easy axes of the film (the dashed lines shown in Fig. 7) depart from the ⟨100⟩

// H

⊥ H

4 μm

(a) (b)

FIG. 8. Foucault images of the Fe(150 Å)/GaAs(001) film for the field applied along the easy axis. The components of induction mapped were parallel and perpendicular to the applied magnetic field direction for reverse field strengths ($H_r \| [010]$) of (a) $H^e_{\rm crit}$, (b) 1.09 $H^e_{\rm crit}$.

directions. However, for the Fe(150 Å)/GaAs(001) film under investigation here, the measured value of the uniaxial anisotropy is smaller than 1% of the cubic anisotropy constant so that deviations from the crystallographic directions are very small.

2. ⟨100⟩ easy directions

The Fe(150 Å)/GaAs(001) film was then rotated through 45° in the microscope so that its [010] direction lay parallel to the field direction. Following a similar procedure to that used for the ⟨110⟩ direction, a single domain state was induced by applying an initial field $H_i = 120$ Oe along $[0\bar{1}0]$. After removal of the field no walls were observed in the sample, as is consistent with the square loop observed by MOKE. Magnetization reversal was then studied by applying successively greater fields parallel to [010]. No change was observed up to a critical field of $H^e_{\rm crit}$ at which point domain walls appeared suddenly ($H^e_{\rm crit} = 7.8$ Oe for the field amplitude $H_i = 120$ Oe). A pair of Foucault images, sensitive to orthogonal induction components and recorded at this field, are shown in Fig. 8(a). It is immediately clear that the domain structures themselves are much more complex than those obtained when fields are applied parallel to ⟨110⟩. The evolution of the domain structure shown in Fig. 8(a) is shown for a field of 1.09 $H^e_{\rm crit}$ in Fig. 8(b). In both cases the structure observed is of the checkerboard type which was also observed in the demagnetized Fe/MgO(100) films.[15,16] The magnetization distributions deduced from the images are shown schematically in Fig. 9 (the magnetization distribution for an intermediate field value 1.07 $H^e_{\rm crit}$ is also shown in Fig. 9). A similar checkerboard domain pattern is formed if the field is applied along [100] rather than [010] as can be seen from the domain schematics in Figs. 10. Increasing the field above 1.13 $H^e_{\rm crit}$ in both cases led to a complete loss of domain walls with the sample returning to a single-domain state, albeit with a reversed magnetization vector.

The main features of the domain structures seen in

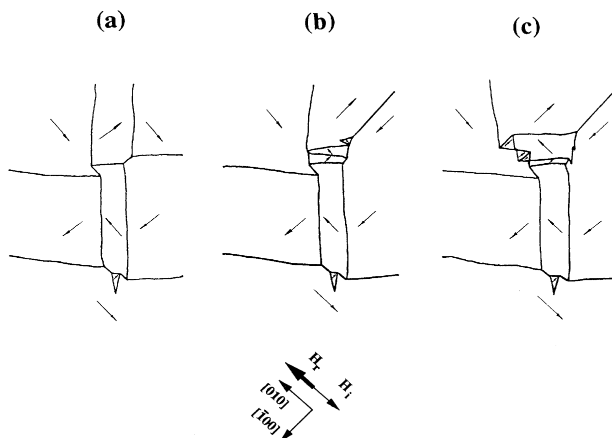

FIG. 9. Schematic diagram of the magnetization distributions deduced from Fig. 8. The reverse field (H_r) strengths (a) $H^e_{\rm crit}$, (b) 1.07$H^e_{\rm crit}$, (c) 1.09$H^e_{\rm crit}$.

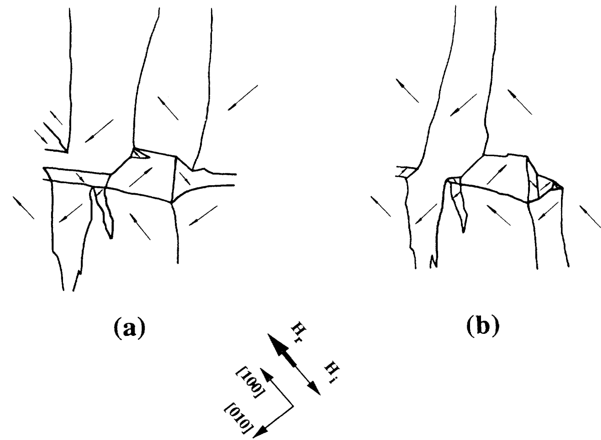

FIG. 10. Schematic diagram of the magnetization distributions deduced from Foucault images of the Fe(150 Å)/GaAs(001) film for the field applied along the second easy axis ($H_r \| [100]$). The reverse field (H_r) strengths (a) $H^e_{\rm crit}$, (b) 1.07 $H^e_{\rm crit}$.

Figs. 9 and 10 can be described as follows. Firstly, domains are present in which the magnetization is oriented along each of the four easy directions expected from the cubic anisotropy. Secondly, the domains have sizes which range from several to a few tens of microns and are generally somewhat irregular in shape. Thirdly, whilst a pure checkerboard domain structure comprises only 90° domain walls [see Fig. 11(a)], some (generally short) 180° walls are observed in our structures. It can be seen that the 90° and 180° domain walls are aligned almost along the ⟨110⟩ and ⟨100⟩ directions, respectively. The 180° domain walls are assumed to arise from the combined action of the applied field and pinning centers: as walls are displaced, some domain walls may be pinned by defects (see Fig. 8) so that the original pure checkerboard domain structure is not maintained and 180° domain walls appear. It does appear that the 180° walls play a significant role in the magnetization reversal process. Indeed, within Figs. 9 and 10 there are examples of how their length can change to facilitate an increase in the size of favorably oriented domains, whilst those in which the magnetization is antiparallel to the applied field shrink. However, as Fig. 11(b) shows, restrictions exist as to where 180° walls can exist and how they can move. Thus an increase in the length of walls with geometries of type *A* lowers the overall energy of the system, those of type *B* are also observed but a change in their length has a very modest effect on the overall energy, whilst type *C* walls simply do not form because of the excessive magnetostatic energy associated with them.

In Figs. 9 and 10, domain-wall displacements are observed clearly. It can be seen that the domain reversal along the ⟨100⟩ direction proceeds mainly via domain-wall displacements. In addition, from a detailed study of Figs. 8 and 9, in domains where the magnetization is perpendicular to the applied field, we observe nucleation and expansion of new domains with magnetization parallel to the applied field thereby increasing the net magnetization

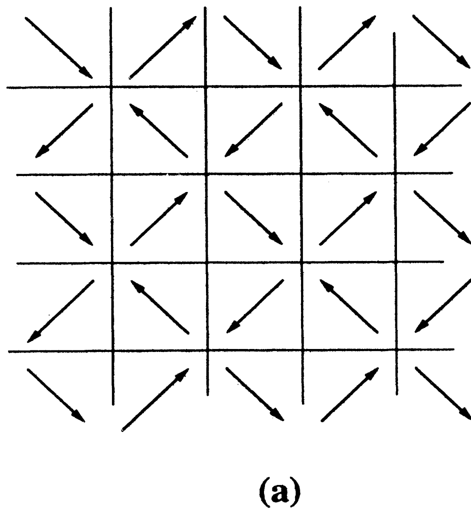

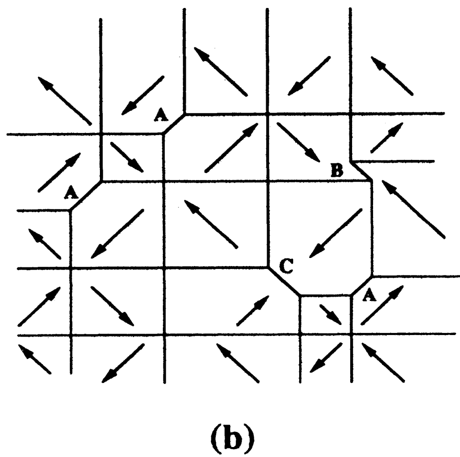

FIG. 11. (a) Schematic representation of a pure checkerboard domain pattern made up of only 90° domain walls, (b) Schematic representation of a checkerboard domain pattern made up of 90° and 180° domain walls.

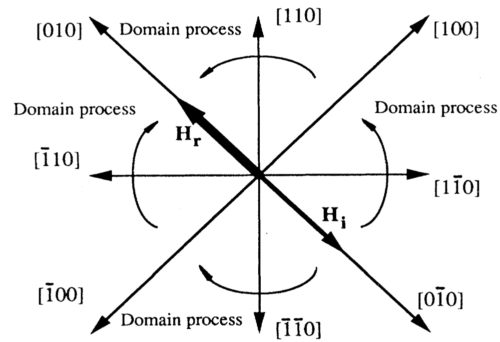

FIG. 12. Magnetization reversal process for applied fields parallel to the ⟨100⟩ direction.

of the sample parallel to the field. However, in the "antiparallel" domains only the nucleation of new domains with magnetization perpendicular to the applied field was observed. Thus, the reversal of the magnetization which is initially antiparallel to the applied field tends to take place not by a single reversal, but by a combination of two 90° changes via an intermediate orientation in which the magnetization lies perpendicular to the applied field direction. This two-step reversal process appears to involve both domain nucleation and wall displacements.

Figure 12 summarizes the main steps in the reversal process when the field is applied along a ⟨100⟩ direction. Since ⟨100⟩ directions are the easy axes for an Fe film with cubic anisotropy, the magnetization should remain oriented along its initial direction (say [0$\bar{1}$0]) when the field is reduced to zero. Even if the applied field is not exactly parallel to the [0$\bar{1}$0] direction, as mentioned in the previous section, during reduction of the field strength to zero, the magnetization will simply rotate to this [0$\bar{1}$0] direction leaving a single-domain remanent state. Ignoring the weak uniaxial anisotropy, the [0$\bar{1}$0] direction is the bisector of another two easy direction, [100] and [$\bar{1}$00], so there should be comparable probabilities for the magnetization to jump into either of these two easy directions as the strength of the field in the [010] direction is increased. Thereafter, further 90° transitions take place to introduce domains in which the magnetization is parallel to the applied field and, over a small field range, all four easy magnetization directions are present in the sample simultaneously. This structure is the checkerboard pattern. It is destroyed by a combination of further domain nucleation and wall motion of the kinds discussed above. For the Fe(450 Å)/GaAs(001) film an irregular checkerboard pattern also develops for reversal along the easy axis direction.

It is significant that all the magnetic domains observed have sizes much larger than the lateral length of surface features revealed by STM. This suggests that the domain size is not affected by the surface topography of these Fe/GaAs(001) films. However, from Lorentz microscopy images, it can be seen clearly that domain walls may be pinned by defects. Thus, the size of domains is mainly determined by the defect pinning. The average defect size and density in our films have been estimated from the TEM images over the window region to be 0.6 μm and 2×10^6 cm^{-2}, respectively. The selected-area electron-diffraction pattern obtained from a defect was always found to be the same as that obtained from GaAs(001) without a capping Fe layer and such defects are not seen in the original GaAs substrate. These suggest that the defects here are noniron inclusions. The simplest explanation is that the defects are pin-holes in the Fe film which cause local contrast similar to that observed at three-dimensional strain centers.[26] On the other hand, in the absence of the defect pinning, it is likely that the domain walls would simply run too rapidly across the film to be observed. Thus, the defects allow the transient domain patterns to be visualized and thus enable the incoherent microscopic reversal processes occurring at very narrow transition fields to be studied. From these studies, distinct microscopic domain processes have been

reproducibly found for reversal along the hard and easy axes.

Finally, in our films the domain walls are fairly straight and have a defined orientation with respect to the crystal axes. This contrasts with the domain structure of ultrathin films with in-plane cubic anisotropy where extremely irregular domain walls develop due to the vanishing magnetostatic contribution to the Néel wall energy in the ultrathin limit.[11,13] Therefore, our results suggest that the 150-Å thickness is sufficient for the magnetostatic part of the wall energy to be important. Nonetheless, the film is still thin enough to be considered as almost a two-dimensional film from the viewpoint of domain formation.

In conclusion, our work shows that a combination of macroscopic MOKE and microscopic Lorentz electron microscopy provides valuable insight into the often complex reversal mechanisms occurring in epitaxial thin films. Distinct microscopic domain processes have been found for reversal along the hard and easy axes. This distinction is associated with the magnetic anisotropy of the films.

ACKNOWLEDGMENTS

We gratefully acknowledge the financial support for this work from the EPSRC, the Toshiba Corporation, and the HCM programme of the EC, and acknowledge helpful discussions with Dr. R. J. Hicken, U. Ebels, Professor G. A. Gehring, Dr. G. A. Prinz, and Professor B. Heinrich. We also thank Dr. D. A. Ritchie, T. River, and L. Zhou for their help with the work.

[1]G. A. Prinz, Science, **250**, 1092 (1990).
[2]G. A. Prinz and J. J. Krebs, Appl. Phys. Lett. **39**, 397 (1981).
[3]J. J. Krebs, B. T. Jonker, and G. A. Prinz, J. Appl. Phys. **61**, 2596 (1987).
[4]G. A. Prinz, B. T. Jonker, J. J. Krebs, J. M. Ferrari, and F. Kovanic, Appl. Phys. Lett. **48**, 1756 (1986).
[5]S. A. Chambers, F. Xu, H. W. Chen, I. M. Vitomirov, S. B. Auderson, and J. H. Weaver, Phys. Rev. B **34**, 6605 (1986).
[6]K. T. Riggs, E. Dan Dahlberg, and G. A. Prinz, Phys. Rev. B **41**, 7088 (1990).
[7]J.M. Florczak and E. Dan Dahlberg, Phys. Rev. B **44**, 9338 (1991).
[8]C. Daboo, R. J. Hicken, D. E. P. Eley, M. Gester, S. J. Gray, A. J. R. Ives, and J. A. C. Bland, J. Appl. Phys. **75**, 5586 (1994).
[9]J. M. Florczak and E. Dan Dahlberg, J. Magn. Magn. Mater. **104**, 399 (1992).
[10]R. Allenspach, J. Magn. Magn. Mater. **129**, 160 (1994).
[11]H. P. Oepen, M. Benning, H. Ibach, C. M. Schneider, and J. Kirschener, J. Magn. Magn. Mater. **86**, L137 (1990).
[12]J. L. Robins, R. J. Celotta, J. Unguris, D. T. Pierce, B. T. Jonker, and G. A. Prinz, Appl. Phys. Lett. **52**, 1918 (1988).
[13]H. P. Oepen, J. Magn. Magn. Mater. **93**, 116 (1991).
[14]H. Sato, R. S. Toth, and R. W. Astrue, J. Appl. Phys. **33**, 1113 (1962).
[15]H. Sato and R. W. Astrue, J. Appl. Phys. **33**, 2956 (1962).
[16]H. Sato, R. S. Toth, and R. W. Astrue, J. Appl. Phys. **34**, 1062 (1963).
[17]E. Gu, E. Ahmad, C. Daboo, S. J. Gray, J. A. C. Bland, L. M. Brown, R. Ploessl, and J. N. Chapman (unpublished).
[18]E. Gu, C. Daboo, J. A. C. Bland, M. Gester, A. J. R. Ives, L. M. Brown, N. A. Stelmashenko, and J. N. Chapman, J. Magn. Magn. Mater. **126**, 180 (1993).
[19]U. Resch, N. Esser, Y. S. Raptis, W. Richter, J. Wasserfall, A. Forster, and D. I. Weatwood, Surf. Sci. **269**, 797 (1992).
[20]C. Daboo, J. A. C. Bland, R. J. Hicken, A. J. R. Ives, and M. J. Baird, Phys. Rev. B **47**, 11 852 (1993).
[21]J. N. Chapman, S. McVitie, and S. J. Hefferman, J. Appl. Phys. **69**, 6078 (1991).
[22]J. N. Chapman, J. Phys. D **17**, 623 (1984).
[23]B. T. Jonker, G. A. Prinz, and Y. U. Idzerda, J. Vac. Sci. Technol. B **9**, 2437 (1991).
[24]D. Jiles, *Introduction to Magnetism and Magnetic Materials* (Chapman and Hall, London, 1991).
[25]C. Daboo, R. J. Hicken, E. Gu, M. Gester, S. J. Gray, E. Ahmad, J. A. C. Bland, R. Ploessl, and J. N. Chapman (unpublished).
[26]P. B. Hirsch, A. Howie, R. B. Nicholson, and D. W. Pashley, *Electron Microscopy of Thin Crystals* (Butterworths, London, 1965).

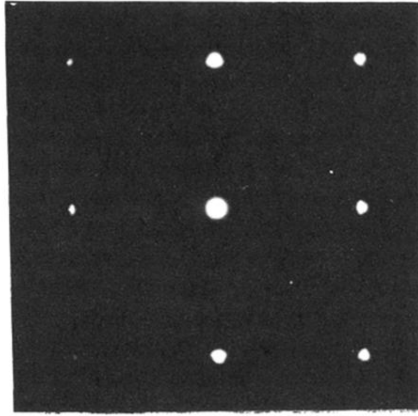

(a)

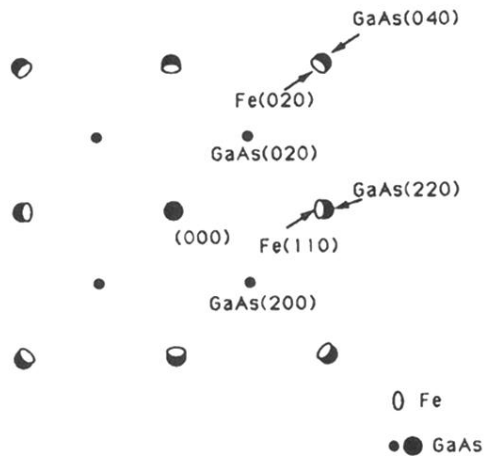

(b)

FIG. 2. (a) A typical selected-area electron-diffraction pattern of Fe/GaAs (001) films, (b) A schematic indexed pattern corresponding to the diffraction pattern shown in (a).

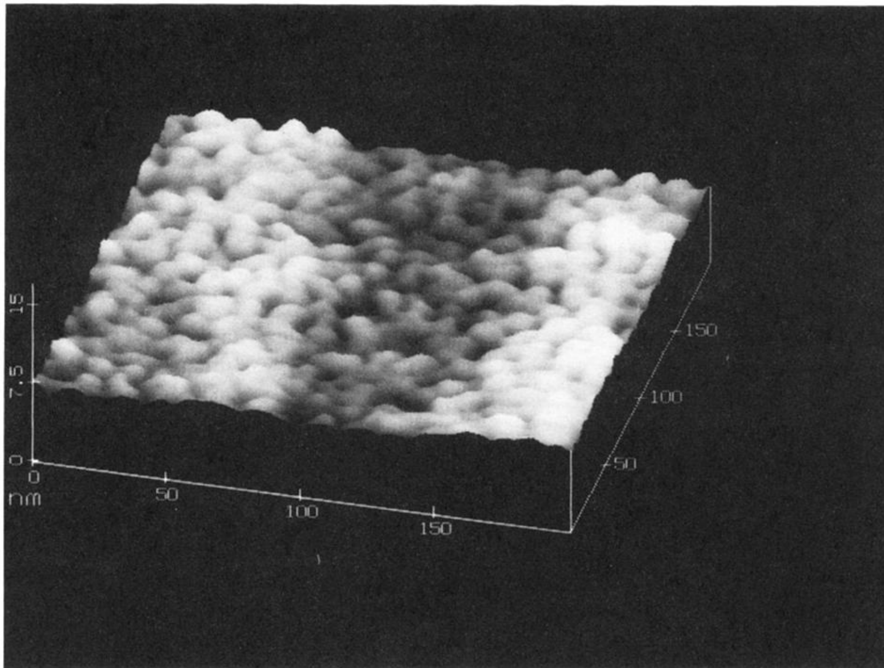

FIG. 3. Scanning tunneling microscope image of an Fe(150 Å)/GaAs(001) film.

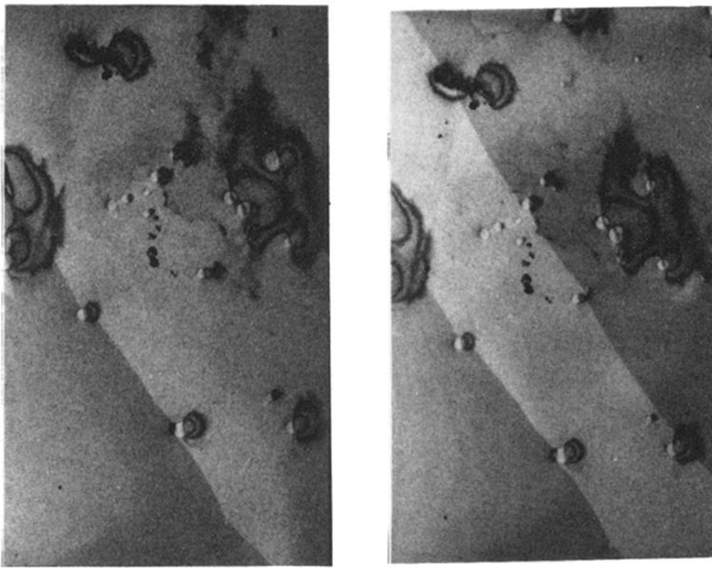

(a) (b)

2 μm

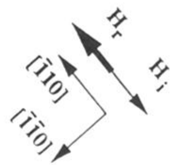

FIG. 5. Foucault images of the Fe(150 Å)/GaAs(001) film for the field applied along the hard axis. The components of induction mapped were parallel to the applied magnetic field direction for reverse field strengths ($H_r \| [\bar{1}10]$) of (a) H^h_{crit}, (b) $1.10 H^h_{\text{crit}}$. Note the defects pinning the domain walls.

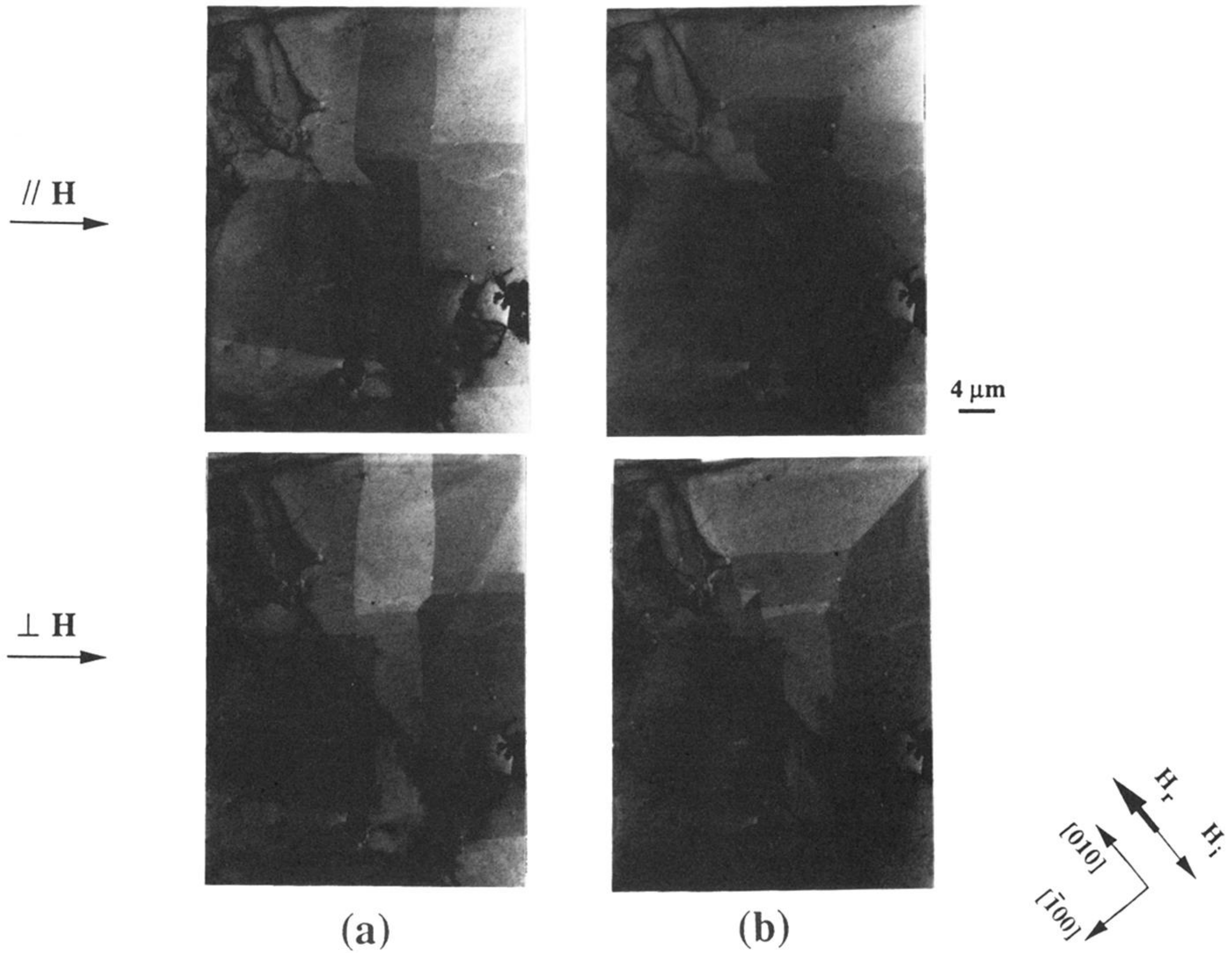

FIG. 8. Foucault images of the Fe(150 Å)/GaAs(001) film for the field applied along the easy axis. The components of induction mapped were parallel and perpendicular to the applied magnetic field direction for reverse field strengths ($H_r \| [010]$) of (a) $H^e_{\rm crit}$, (b) 1.09 $H^e_{\rm crit}$.